JOURNAL OF GEOPHYSICAL RESEARCH, VOL. 88, NO. A11, PAGES 8971-8984, NOVEMBER 1, 1983

Voyager Plasma Wave Measurements at Saturn

F. L. SCARF

Applied Technology Division, TRW Space and Technology Group, Redondo Beach, California 90278

D. A. GURNETT AND W. S. KURTH

Department of Physics and Astronomy, University of Iowa, Iowa City, Iowa 52242

R. L. POYNTER

Jet Propulsion Laboratory, California Institute of Technology, Pasadena, California 91109

The entire set of Voyager plasma wave observations at Saturn is summarized and attention is focused on several specific problem areas. The topics that are emphasized include (1) the size and location of the Saturn foreshock, (2) possible detection of the Jovian magnetic tail after the Saturn encounter, (3) pitch angle scattering of electrons by equatorial whistler mode emissions, and (4) the detection of dust impact signals near the ring plane and at other locations in the magnetosphere.

1. INTRODUCTION

The plasma wave instruments on the Voyager 1 and 2 spacecraft provided direct measurements of low-frequency waves in the magnetospheres of Jupiter and Saturn, but because the encounter conditions and the magnetic latitude profiles were significantly different at the two planets, there are noteworthy differences in the resultant science return. At Jupiter, the large inclination of the magnetic field insured that the Voyagers would have very many crossings of the magnetic equator where some of the strongest magnetospheric wave-particle interactions commonly develop, but since the Saturn magnetic dipole axis is aligned with the planetary spin axis, there were only a total of three Voyager 1 and 2 crossings of Saturn's magnetic equator, and large sections of these encounters involved high-latitude plasma phenomena. The Voyager 2 Saturn flyby was also unusual because at that time the solar wind pressure was low and variable, and the Saturn system was nearly lined up with Jupiter's extended magnetic tail. Other unique characteristics of these encounters involved the very close flybys of both Titan (Voyager 1) and the outer edge of the visible rings (Voyager 2). Finally, a large difference in the overall science return from the two outer planet magnetospheres stems from the disparity in the number of 48-s long wideband plasma wave transmissions; although eighty-four wideband frames were obtained within Saturn's magnetosphere, this number is far less than the corresponding total of 12,000 frames transmitted back from Jupiter.

In this report, we summarize the entire set of Voyager plasma wave observations at Saturn, and we focus attention on several significant results that have not previously been discussed in detail. The specific topics that are emphasized here are (1) The overall extent of the solar wind-Saturn interaction region, (2) pitch angle scattering of electrons by equatorial whistler mode emissions, and (3) the detection of dust impact signals near the ring plane and at other locations in the magnetosphere.

2. MEASUREMENT CHARACTERISTICS AT SATURN

Each Voyager plasma wave system uses a balanced electric dipole antenna with a 7-m effective length. The wave output is processed by a 16-channel analyzer covering the range from 10 Hz to 56 kHz and by a wideband receiver covering the range from 50 Hz up to about 14 kHz. The 16-channel analyzers have only two logarithmic compressors for the full spectral coverage, and there is no peak detection or sample and hold capability. For the planetary encounters, a full 16-channel spectral scan is completed once every 4 s.

The wideband receiver system has an automatic gain control (AGC) amplifier and a four-bit analog-to-digital converter to interface with the Voyager high rate telemetry link normally assigned to the imaging system. The output of the waveform amplifier is intermittently sampled at a rate of 28,800 words per second in 48-s intervals or frames, with each frame containing 800 successive 60 ms subsequences. The 28,800 word per second sampling rate leads to a 35-μs time between samples, and in order to avoid signal aliasing, the input circuit has a filter that rolls off strongly about 12 kHz, but very intense high-frequency signals are detected up to the Nyquist frequency of 14.4 kHz. Other aspects of the instrument design are discussed in a report by *Scarf and Gurnett* [1977], and details of the measurements at Jupiter are discussed in a paper by *Scarf et al.* [1981*a*].

At an early stage, the Voyager project decided that the spacecraft interface with the wideband system would be designed to operate only at the 115-kbit/s rate, and this fact led to a major problem for all of the more distant planetary encounters. During the Jupiter flybys, the spacecraft transmitted directly to earth at the 115 kbit/s rate so that the wideband plasma wave spectra could be telemetered in real time while images were being sent to the spacecraft tape recorder, or the situation could be reversed. However, Voyager was never able to transmit 115 kbit/s of data over the great distance from Saturn to earth, and so the real time transmissions necessarily involved imaging formats or tape recorder playbacks that were able to operate at lower telemetry rates. Since the wideband plasma wave output required 115 kbit/s, the data had to be placed on the tape recorder for subsequent slow playback. Thus, at Saturn the plasma wave wideband measurements were in competition for very restricted space on the tape recorder, and each frame required a playback interval that was considerably longer than the 48-s measurement time.

These serious operational difficulties were addressed by the Voyager sequence design teams, and every effort was made to find useful slots where wideband plasma wave measurements

Paper number 3A0489.
0148-0227/83/003A-0489$05.00

TABLE 1. Number of Plasma Wave Wideband 48-s Frames Per Day at Saturn

Date (Day)	Number
Voyager 1 (1980)	
November 11 (316)*	0
November 12 (317)	11
November 13 (318)	9
November 14 (319)	4
November 15 (320)	8
November 16 (321)†	2
Total:	34
Voyager 2 (1981)	
August 24 (236)*	4
August 25 (237)	6
August 26 (238)	16
August 27 (239)	6
August 28 (240)	6
August 29 (241)	6
August 30 (242)	6
August 31 (243)†	0
Total:	50

*After first bow shock crossing
†Before last bow shock crossing

could be placed on the tape recorders. This effort yielded a total of 84 frames in Saturn's magnetosphere for an average of six frames a day, as shown in Table 1. (*Scarf et al.* [1981*a*] noted that at Jupiter the corresponding totals were 12,071 frames with an average of 223 frames per day. However, most of these Jupiter wideband frames were transmitted as unscheduled substitutes for certain imaging frames.)

3. The Saturn-Solar Wind Interaction

Gurnett et al. [1981*a*] and *Scarf et al.* [1982] presented initial descriptions of the Voyager 1 and 2 plasma wave measurements at Saturn, and they focused attention on the relatively short intervals between the initial inbound traversals of the bow shock and the final outbound shock crossings. Figure 1 shows the relevant Voyager 1 and 2 encounter trajectories in rotated planet-centered, sun-oriented coordinates, and the large dots mark the most distant bow shock traversals. Discussions of the magnetic field and plasma profiles near these shock crossings are contained in companion reports by *Ness et al.* [1981, 1982] and *Bridge et al.* [1981, 1982]; *Scarf et al.* [1981*b*] also discussed these measurements in a report on bow shock microstructure at four planets.

Figure 1 indicates that the Voyager 2 measurements of inbound shock locations were generally consistent with the Voyager 1 result, but the dashed curve in Figure 1 clearly fails to join the two sets of outbound observations by a very wide margin. Several of the reports cited above contain speculations that during the Voyager 2 outbound leg there were large variations in solar wind pressure leading to very distant final shock crossing positions. Several of the Voyager 2 reports also contained speculations that the large size of the magnetosphere during the Voyager 2 outbound leg was associated with immersion of the Saturn system in the magnetic tail of Jupiter. In this section, we examine this possibility by considering Voyager plasma wave measurements for an extended region surrounding the Saturn encounters.

Scarf [1979] first noted that the Voyager 2 encounter would occur when Saturn was nearly aligned with the Jupiter-sun line, and he suggested that Saturn's magnetosphere might intermittently be within the Jovian tail during the encounter period. Evidence that Voyager 2 did traverse Jupiter's distant magnetotail on its way to Saturn has been presented by *Scarf et al.* [1981*c*], *Kurth et al.* [1981*b*, 1982*b*], and *Lepping et al.* [1982], and recently *Kurth et al.* [1982*a*] showed that weak continuum radiation detected at Saturn had characteristics very similar to the corresponding emissions from the Jupiter tall region.

The waveform data are useful for the identification of continuum radiation, and the top panel in Plate 1 contains a color-coded frequency-time spectrogram of particular interest. (Note: Plate 1 is shown here in black and white. The color version is shown in a separate section of the journal.) These measurements were made just upstream from Saturn, and an enhanced black and white display for a reduced frequency range was also shown by *Kurth et al.* [1982*a*]; the very weak broadband emission with a lower cutoff near 3.5 kHz was labeled 'Jovian continuum radiation' by Kurth et al., and the authors conjectured that Saturn was in a moderately low-density region surrounding the extended Jovian tail just before the Voyager 2 encounter. In order to obtain further information on the proximity to the Jovian tail, it is necessary to search for such tail effects in the post-encounter region, since in Saturn-centered coordinates, the gravity assist moved Voyager 2 back toward the direction of the Jupiter-sun line (J. Eberhart, (private communication, 1979) was the first to note that this deflection would suggest a search for Jupiter tail phenomena in the post-encounter data set).

The analysis of Voyager plasma wave measurements in the region beyond the outbound bow-shock surface is also of interest because for Saturn, this is the region of the foreshock [*Greenstadt and Fredricks*, 1979] where suprathermal electrons from the shock flow away parallel to the magnetic field, producing electron plasma oscillations (see, for instance, *Scarf et al.* [1971] and *Anderson et al.* [1981]). Figure 1 shows the nominal hose angle at 9.25 AU, and this indicates that Voyager 2, in particular, should have been in the foreshock for an extended interval. To demonstrate how big the Saturn foreshock region actually is, we show in Figure 2 Voyager 1 and 2 plasma wave data covering the frequency channels for normal electron plasma oscillations at 9.25 AU [$f \approx 1.8$–5.6 kHz, corresponding to $N_e \approx 0.04$ to 0.4 electrons/cm^3]. In each case, the plots start one week before closest approach and include a total of 43 days, and the measurements represent peaks and averages for 19.2-min intervals.

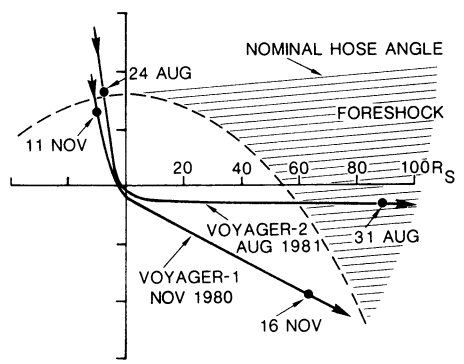

Fig. 1. Voyager 1 and 2 trajectories in cylindrical sun-oriented coordinates. The distance units are in Saturn radii, and the dots show the positions of the initial and final bow shock traversals for Voyagers 1 and 2. The dashed curve approximates a mean shock surface, and the foreshock boundary is drawn for a nominal hose angle field orientation.

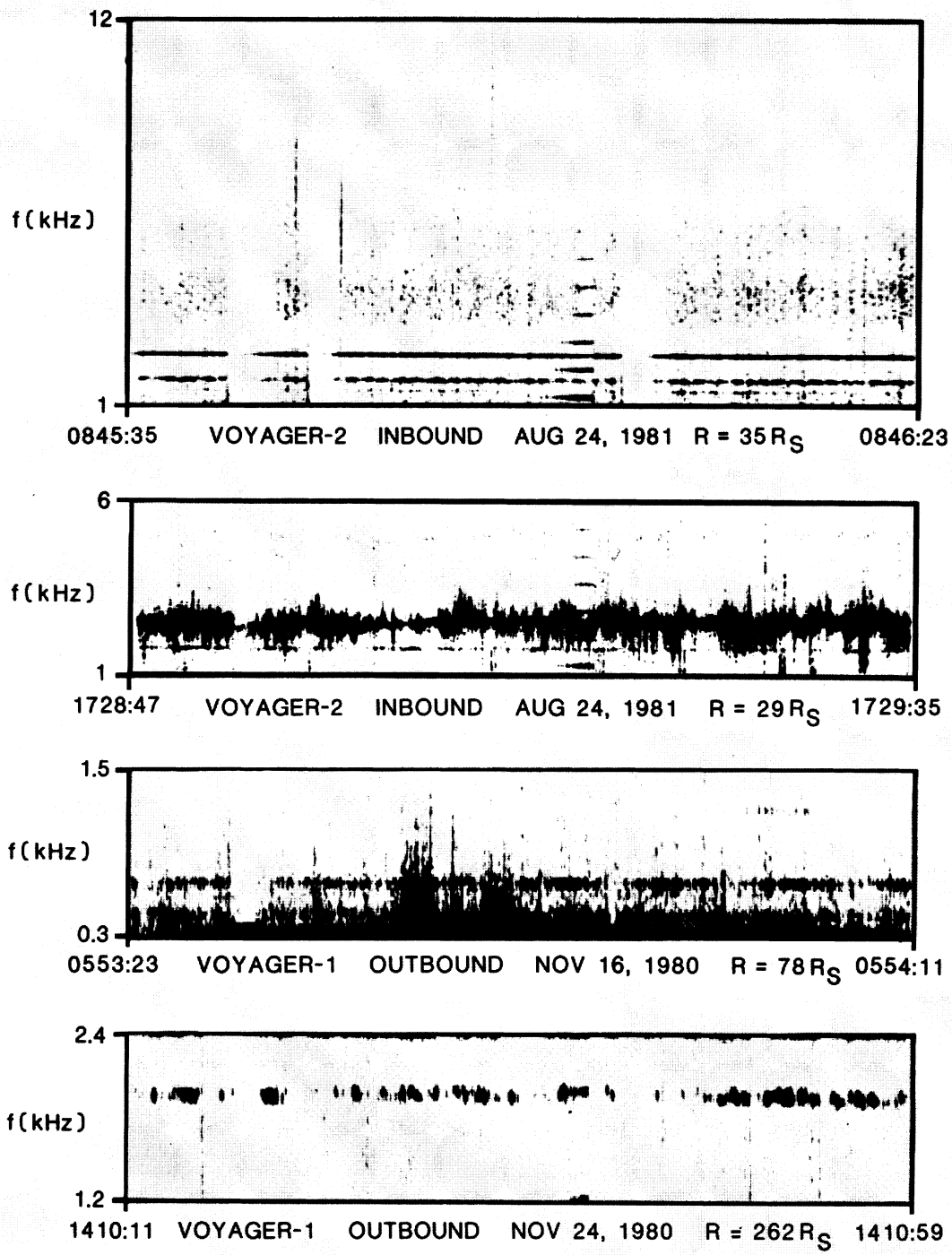

Plate 1. Frequency-time diagrams made up from the wideband measurements. The top panel shows weak continuum radiation similar to that detected at Jupiter, and this may indicate that Saturn was near the Jovian tail during the Voyager 2 encounter. The second and bottom panels show electron plasma oscillations, and the other panel shows ion acoustic waves detected at the beginning of the Voyager 1 outbound bow shock traversal.

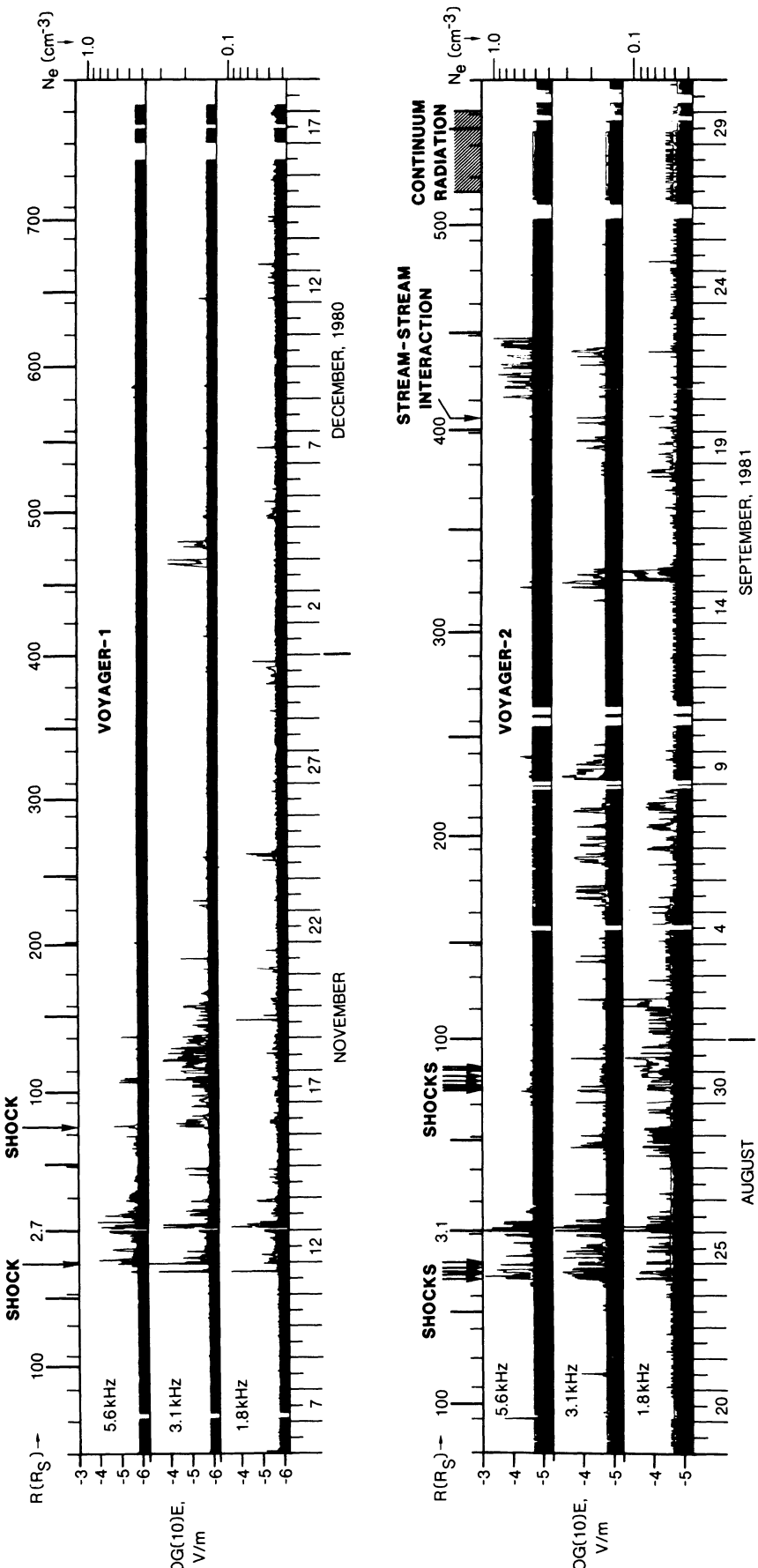

Fig. 2. Wave amplitudes for the nominal electron plasma oscillation channels near Saturn. The plotted points are peaks and averages over 19.2 minutes, and the electron density scale is shown on the right. The Saturn encounters are contained in the relatively brief segments between bow shock crossings, and the extensive turbulence after the final outbound crossings represents traversal of the Saturn foreshock. The continuum radiation detected late in September 1981 is similar to that detected earlier in the low-density region surrounding the Jovian tail.

It can be seen from Figure 2 that essentially no plasma oscillations were detected before the encounters, and this result is consistent with expectations for the nominal field orientation drawn in Figure 1. On Voyager 2, the only intense 'upstream' electron plasma oscillations were detected from 1708 to 1831 on August 24, 1981, between the second and third encounters with the bow shock; at 1728 : 47, a 48-s long wideband frame was recorded, and the frequency-time spectrogram for these strong and fairly continuous emissions is shown in Plate 1. The bottom panel in Plate 1 shows the more customary electron plasma oscillation profile in the post-encounter foreshock; this has a series of discrete noise bursts that provide low average wave levels but large peak values.

We note from Plate 1 and from Figures 1 and 2 that the final outbound shock crossing on Voyager 1 occurred on November 16, 1980, at a distance of 78 R_s and that Voyager 1 had moved 184 $R_s = 1.1 \times 10^7$ km farther away from Saturn by November 24, when these nearly final foreshock electron plasma oscillations were detected. As expected from the trajectory plot, Figure 2 demonstrates that Voyager 2 detected foreshock electron effects over a much larger region, extending at least out to 350 R_S ($=2.1 \times 10^7$ km ≈ 0.15 AU) beyond the bow shock. In fact, for Voyager 2, we continued to detect intermittent bursts of electron plasma oscillations out to more than twice this distance, suggesting that in late 1981 the Saturn foreshock had an enormous extent. It is noteworthy that at earth foreshock electron plasma oscillations are generally detected only out to about 30–60 $R_E \approx 2$–4×10^5 km [*Scarf et al.*, 1971; *Greenstadt and Fredricks*, 1979; *Anderson et al.*, 1981].

The existence of this huge region affected by a strong interaction between the solar wind and Saturn's magnetosphere could have been related to the nearby presence of the Jovian tail, and Figure 2 identifies a three-day period (September 27, 28, 29, 1981) when weak Jupiter-like continuum radiation was actually detected by the Voyager 2 plasma wave instrument. Some 96-s peaks and averages are displayed in Figure 3 for several mid-frequency plasma wave channels. The steady peaks at 1.0 and 1.8 kHz are artificial (they represent effects of repetitive spacecraft interference phenomena, as discussed by *Scarf et al.* [1981*a*]), but the varying average level at 1.78 kHz has characteristics essentially identical to those of the signals designated as continuum radiation surrounding the distant magnetic tail of Jupiter [*Scarf et al.*, 1981*c*; *Kurth et al.*, 1981*b*, 1982*b*]. During this period, the Voyager 2 plasma probe measured very low densities [*Lazarus*, 1982], and the combined results are consistent with a post-Saturn encounter with the wake region surrounding the central part of the extended Jovian tail.

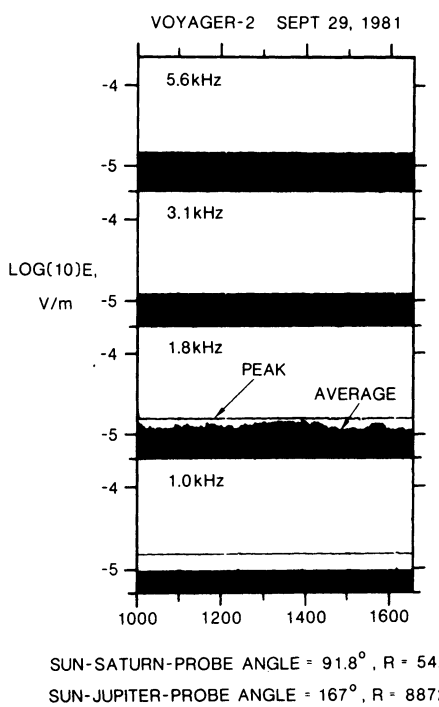

Fig. 3. Expanded display of the continuum radiation. Peaks and averages measuring 96 s are shown. The 1.8-kHz peak remains high and steady because of a spacecraft interference effect.

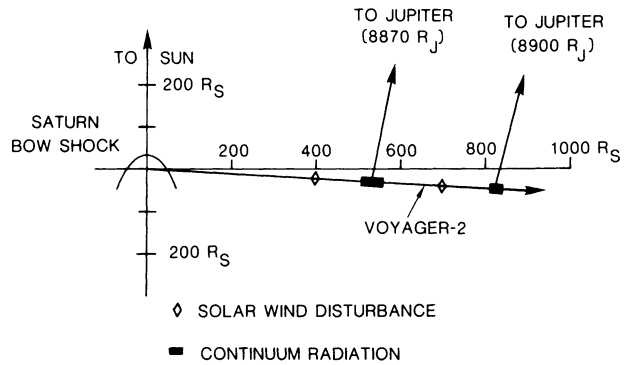

Fig. 4. The post-encounter trajectory of Voyager 2 in Saturn-centered sun-oriented coordinates.

It is of interest to note that this apparent tail encounter occurred roughly one week after passage of a shocklike interplanetary disturbance (the September 20 event labeled 'stream-stream interaction' in Figure 2). An interplanetary shock was also detected on October 10, 1981, and on October 17 there was another tail-like encounter with weak 1.8-kHz continuum radiation and low plasma probe densities. (A third and final post-Saturn tail encounter occurred on October 30 when Voyager was at a distance of 8926 R_J from Jupiter.) Figure 4 shows the extended trajectory of Voyager 2 with respect to Saturn, and the spacecraft positions for these solar wind and tail-encounter events are marked, along with the directions to Jupiter. It appears likely that low and variable solar wind pressures that frequently develop a week or so after passage of an interplanetary shock could allow the Jovian tail to expand and move from the normal direction, as discussed by *Kurth et al.* [1982*b*]. It is also interesting to speculate that the existence of such an enormous detectable foreshock region after the Voyager 2 encounter might be related to the presence of the Jovian tail within the foreshock. That is, some electrons streaming out along the interplanetary magnetic field could be reflected and even accelerated by irregularities associated with Jupiter's tail.

4. Magnetospheric Wave Measurements

Scarf et al. summarized all of the Voyager 1 and 2 spectrum analyzer measurements at Jupiter in a single long drawing (*Scarf et al.* [1981*a*], pages 8185, 8186) that contained profiles of 4.8-min averages for each of the 16 bandpass channels. This drawing had data for 58 days, and it showed that there were very few places in Jupiter's magnetosphere where low plasma wave levels were detected.

Figure 5 contains the equivalent spectrum analyzer plots for the Saturn magnetosphere traversal. The labels 'S' and 'M' refer to crossings of the bow shock and the magnetopause, 'T' refers to the Voyager 1 Titan flyby (see *Gurnett et al.* [1981*a*, 1982*a*]), and '$\theta = 0°$' marks the crossing of Saturn's ring plane and

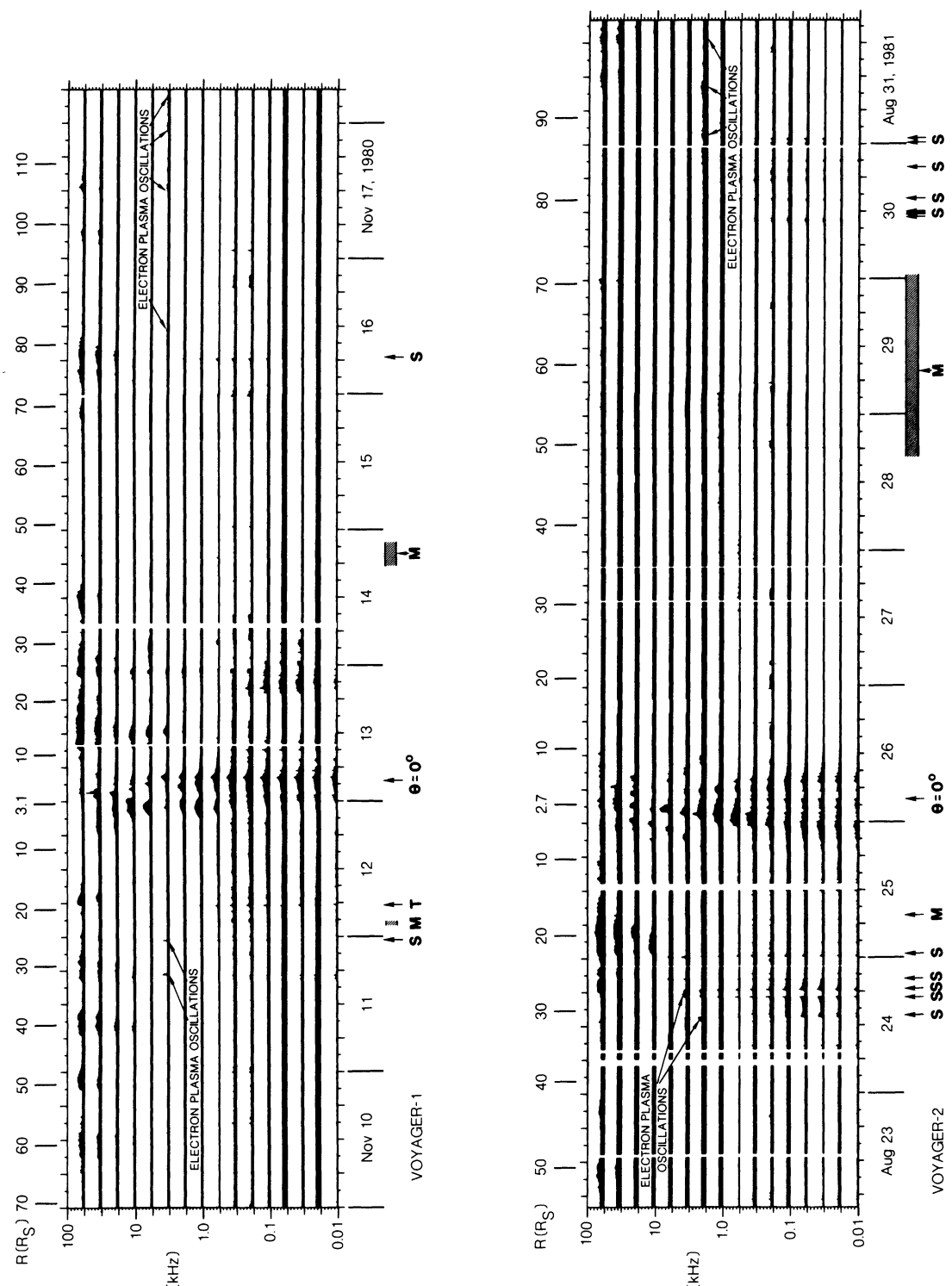

Fig. 5. A summary of all Voyager 16-channel spectrum analyzer measurements within Saturn's magnetosphere. The plotted points are 4.8-min averages, and the labels 'S,' 'M,' and 'T' represent crossings of the bow shock, the magnetopause, and the Titan wake, respectively.

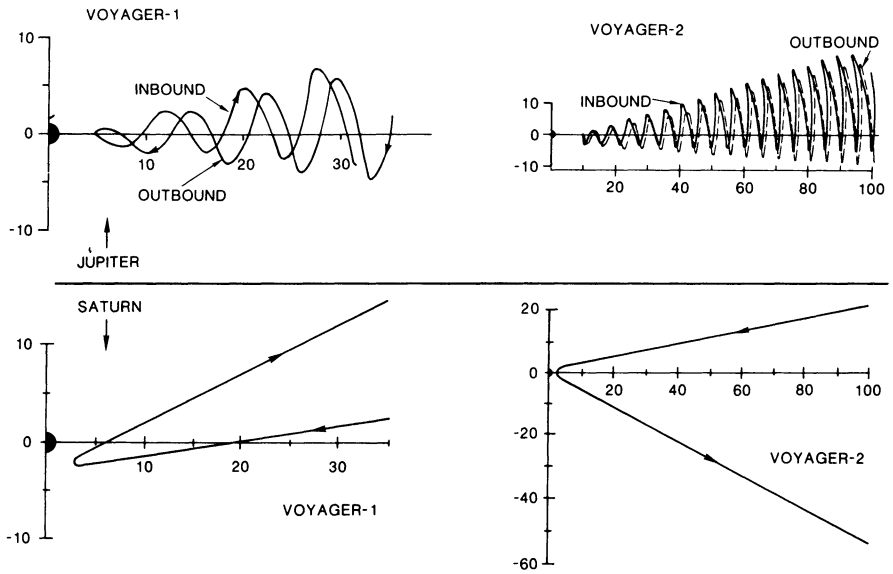

Fig. 6. Comparison of the Voyager 1 and 2 flybys of Jupiter and Saturn in terms of radius versus magnetic latitude plots. It can be seen that the Saturn encounters were basically high-latitude traversals.

magnetic equator. The 4.8-min averages for the electron plasma oscillations are labeled to demonstrate how difficult it is to identify these emissions in a plot of average amplitude values; the impulsive nature of these bursts can best be appreciated by comparing the displays in Figures 2 and 5 for the same channels and the same days. It is even more striking that the intense waves detected at the bow shock crossings and at Titan [*Gurnett et al.*, 1981*a*; *Scarf et al.*, 1982] are virtually not visible in this average plot; these waves are also highly impulsive.

Figure 5 also shows that the most intense wave activity was strongly concentrated in the one- to two-day intervals centered at closest approach, and this figure differs greatly from the corresponding plot in the Jupiter summary paper [*Scarf et al.*, 1981*a*]. In particular, Figure 5 shows that there were lengthy periods within the Saturn magnetosphere when very low wave levels were detected in all channels below 10 kHz (the 10- to 56-kHz signals are the low end of the Saturn kilometric radio spectrum, and a 10.66-hour modulation represents the rotation of Saturn's magnetic field [*Desch and Kaiser*, 1981]; at low frequencies, the actual modulation is irregular because it is affected by the orbital phase of Dione [*Gurnett et al.*, 1981*a*; *Kurth et al.*, 1981*a*; *Desch and Kaiser*, 1981]).

One reason for this difference in appearance is connected with the fact that the continuum radiation detected within Saturn's magnetosphere has a spectral density at least two orders of magnitude lower than that of the corresponding Jovian emission [*Kurth et al.*, 1982*a*]. A second important source of the difference involves the great disparity between the Voyager magnetic latitude profiles during the encounters at Jupiter and at Saturn. This is illustrated in Figure 6 where magnetic latitude versus radius plots for portions of the Voyager 1 and 2 Saturn encounters (bottom) are compared with scaled versions of the corresponding Jupiter plots (top).

Here it can readily be seen that since the Saturn magnetic dipole is aligned with the spin axis, these encounters basically involved high magnetic latitudes; thus, the Saturn magnetic equator was crossed only twice by Voyager 1 (at the orbits of Titan and Dione) and once by Voyager 2 (at 2.77 R_S). On the other hand, the large tilt of the Jovian magnetic field with respect to Jupiter's spin axis provided a very significant opportunity to scan regularly in magnetic latitude, and the top part of Figure 6 clearly shows how the Voyager Jupiter traversals involved repeated crossings of the magnetic equator. Since many classes of wave-particle interactions develop maximum strength near the magnetic equator, and since the plasma tends to be confined in a disc or torus near the centrifugal equator, it is not really surprising that, in the absence of intense trapped continuum EM radiation, the Voyager plasma wave activity was strongest in the low-latitude regions near closest approach to Saturn.

The initial reports by *Gurnett et al.* [1981*a*] and *Scarf et al.* [1982] contained 24-hour plots of the Voyager 1 and 2 16-channel spectrum analyzer observations centered about the times for closest approach. In each case, local values of the electron cyclotron frequency (f_c[Hz] = 28 B [gamma]) were derived from the magnetometer measurements [*Ness et al.*, 1981, 1982], and f_c profiles were plotted along with the wave data. For Voyager 1, Gurnett et al. also provided a preliminary estimate of the electron plasma frequency profile (f_p[kHz] = $9[N]^{1/2}$, with N in cm^{-3}), derived largely from initial interpretations of the variations in wave intensity levels. A reanalysis of some high-frequency wave measurements by *Pederson et al.* [1981] suggested modifications in this density profile, and subsequent detailed studies by members of the Voyager plasma science team yielded greatly improved local density estimates. However, the available plasma probe results are still somewhat preliminary because the presence of very cold electrons, as well as effects associated with spacecraft charging, deviations in ion flow direction, and variations in ion composition introduce data analysis problems that are not easily resolved. Nevertheless, the electron measurements yield straightforward lower bounds for N, and these lower bounds, provided by the Voyager plasma team [A. Lazarus, private communication, 1982; *Sittler*, 1982], were used to construct new f_p profiles that are shown in Figures 7 and 8.

For the first ten-hour period on November 13, the f_p profile in Figure 7 differs considerably from the preliminary one shown by *Gurnett et al.* [1981*a*]. Since plasma wave modes are identified by comparing the wave frequencies with local values for f_p and f_c, it is appropriate to review the Voyager 1 analysis by using the new density curve. We note that at low frequencies ($f \leq 1.0$ kHz) the intense wave activity in Figure 7 has $f < f_c$,

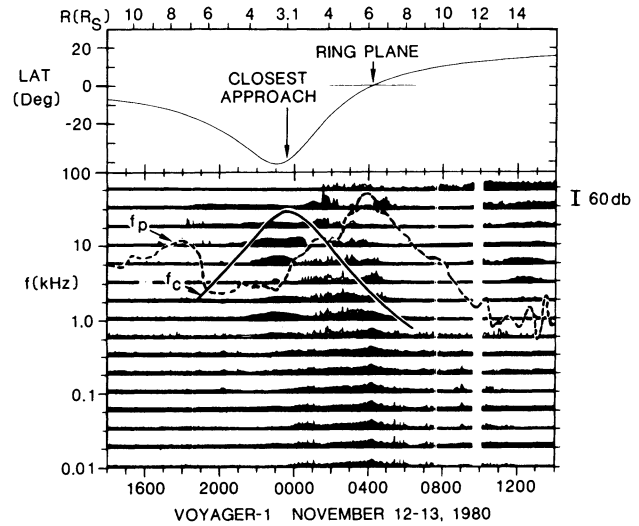

Fig. 7. Voyager 1 16-channel spectrum analyzer observations for the 24-hour interval centered about closest approach. The f_c curve is derived from magnetometer data and the f_p curve, derived from the plasma electron measurements, may represent a lower bound.

$f \ll f_p$, and it is peaked near the magnetic equator (ring plane crossing) with a secondary maximum near closest approach. *Gurnett et al.* [1981*a*] designated these emissions as 'hiss and chorus,' and this whistler mode identification is not affected by the changes in f_p. Similarly, the '$(n + \frac{1}{2})f_c$ band' designation for the 3-kHz enhancement near 0430 and the 5.6 kHz burst at 0300, as well as the 'radio emission' designation for the high-frequency waves (3.1 kHz $\leq f \leq$ 56 kHz) detected after 1000 are unaffected by the change in the density curve. However, the new f_p profile is not in accord with some of the other identifications noted in the preliminary discussion by *Gurnett et al.* [1981*a*], particularly for the intervals near 0100–0200 (November 13) and 1800–2230 (November 12).

The initial Voyager 1 plasma wave report contained the following analysis for the November 12 interval: (1) brief noise bursts were detected in the 10-kHz and 17.8-kHz channels between 1800 and 2000, and these impulsive events had characteristics of electron plasma oscillations; (2) past 2000 a band of intense steady emissions was identified with a well-defined lower cutoff that first decreased smoothly from 10 kHz ($\approx$ 2030) down to 3 kHz ($\approx$ 2300) and then increased. These waves were identified as electromagnetic, and it was natural to assume that the smoothly-varying lower cutoff represented a propagation cutoff at the local value for f_p.

A Voyager 1 wideband frame was recorded at 2252 on November 12, and it showed that this radio emission had a very unusual spectral structure, containing a sequence of many narrowband emissions rather than the expected continuum. *Gurnett et al.* [1981*b*] used data from several additional wideband frames to show that the narrowband electromagnetic emissions were detected sporadically out to 59 R_S during the outbound leg, and it was suggested that the waves were generated by conversion of intense electrostatic waves to electromagnetic emissions in inner magnetospheric regions with strong density gradients. More recently, *Gurnett et al.* [1982*c*] analyzed Voyager 1 wideband data showing similar narrowband emissions at Jupiter, and this generation process appears to be a common one.

The f_p profile shown in Figure 7 does not explain the impulsive noise bursts between 1800 to 2000 on November 12, or the low-frequency cutoff of the narrowband emissions between 2000 and 2300. Moreover, on the basis of experience in the earth's magnetosphere, *Gurnett et al.* [1981*a*] identified the very intense 31-kHz noise burst at 0130 (November 13) as an upper hybrid resonance emission, but this identification is also quite inconsistent with the f_p profile in Figure 7. It is possible that (unmeasured) cold electrons were present in sufficient numbers to yield significantly higher total densities, but it is also possible that other interpretations are appropriate for these specific wave phenomena that were readily explained only when the initial f_p curve was used [see *Kurth et al.*, this issue].

It is known that very cold electrons had to be present during a part of the Voyager 2 encounter. Specifically, at the ring plane crossing, a high ion density was detected [*Bridge et al.*, 1982], but the measured electron density was low [*Lazarus*, 1982]. Thus, the f_p curve in Figure 8 gives only a lower bound near the equator. However, for Voyager 2 there appear to be no serious problems associated with the new f_p profile. For instance, *Scarf et al.* [1982] used upper hybrid resonance identifications to derive $f_p \approx 5.6$ kHz at 1640–1700, $f_p \cong 10$ kHz (2040–2120), and $f_p \approx 18$ kHz at 2235–2315, and these values agree reasonably well with minimum values derived from the Voyager 2 plasma probe. Moreover, the Voyager 2 detection of intense narrowband emissions at 5.6 kHz started just after 0202, and this onset occurred fairly soon after a drastic dip in f_p. Thus one might relate the emission onset to the spacecraft motion into a propagation region where the local cutoff frequency was below the wave frequency.

Figure 8 also shows Saturn kilometric radiation, $(n + \frac{1}{2})f_c$ bands, and whistler mode chorus and hiss. Detailed discussions of the electrostatic waves are contained in a report by *Kurth et al.* [this issue]. In the next sections of this paper, we discuss in more detail the whistler mode emissions and the Voyager detection of dust impacts in Saturn's magnetosphere.

5. Chorus and Electron Scattering

Figure 9 illustrates in detail how the 16-channel wave levels varied during the Voyager 1 ring plane-magnetic equator crossing. Here the calibrated and unaveraged field amplitudes are plotted, and the new f_p curve (based on the *Pedersen et al.* [1981] analysis and the electron plasma probe measurements (A. Lazarus, private communication, 1982; E. C. Sittler, private communication, 1982)) is again superimposed. The f_c, $3f_c/2$,

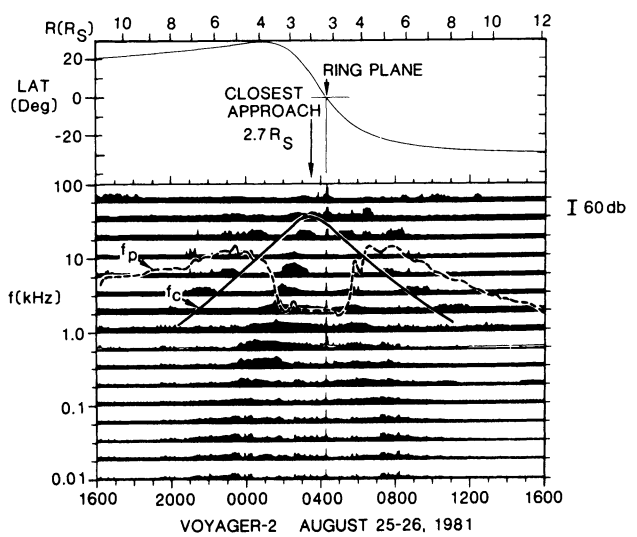

Fig. 8. Same format as Figure 7 for Voyager 2.

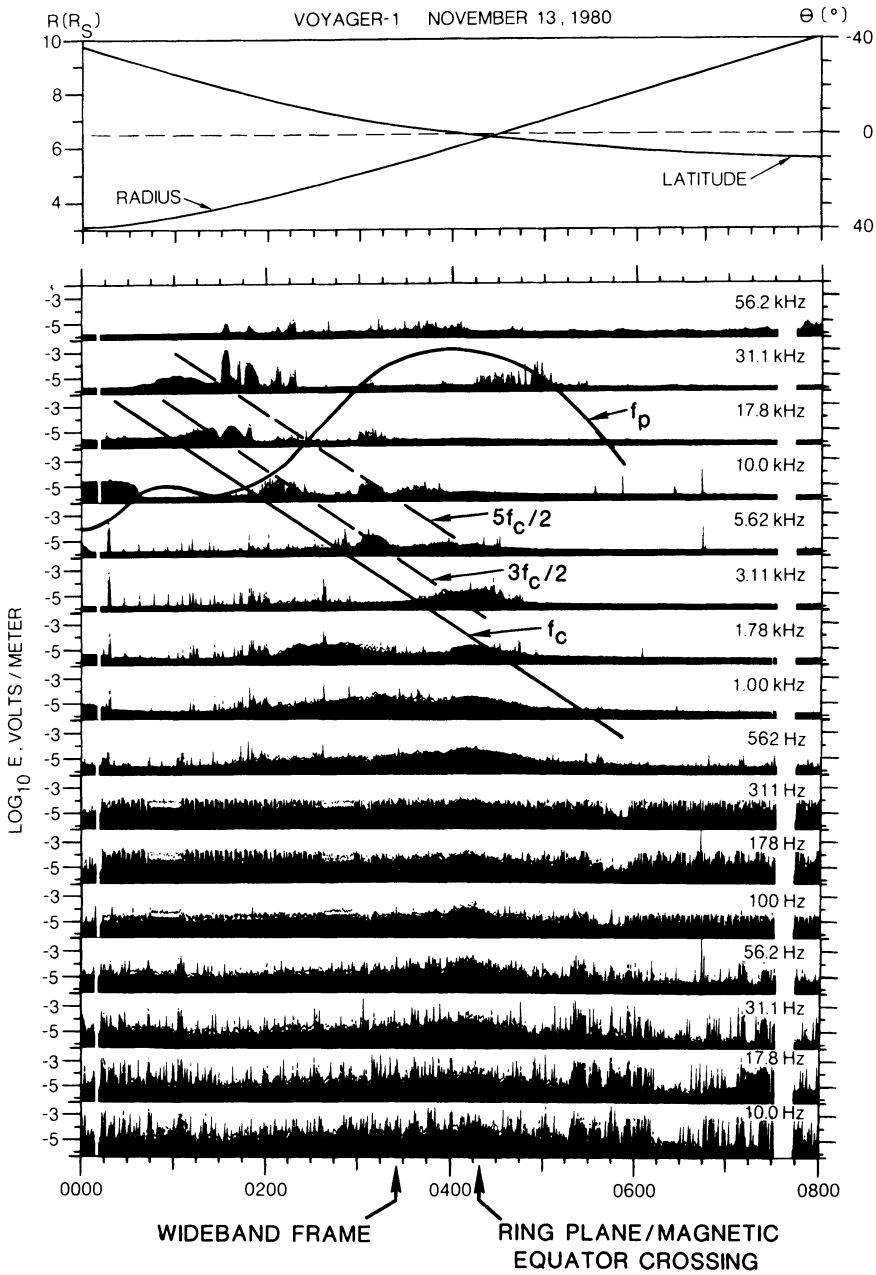

Fig. 9. Detailed plot of the Voyager 1 spectrum analyzer measurements near the outbound crossing of the ring plane and magnetic equator.

and $5f_c/2$ curves generally serve to order the high-frequency noise bursts in terms of $(n + \frac{1}{2})f_c$ bands, but it seems clear that between 0100 and 0230, the variations in the 17.8-, 31-, and 56-kHz channels cannot be completely explained in terms of ordinary electron gyroharmonics.

At 0326 a wideband frame was recorded, and the full color-coded spectrogram was displayed by *Gurnett et al.* [1981*a*], who showed that weak electron gyroharmonic bands and strong hiss and chorus were present. The 48-s long spectrogram is actually made up of 800 successive spectral scans, and Figure 10 contains a 0.6-s average of ten of these scans. This plot shows clearly that three fairly weak $(n + \frac{1}{2})f_c$ emissions were detected along with strong banded chorus and somewhat weaker hiss. The term 'chorus' is used because the waves are banded with $f \lesssim f_c/2$, and they have characteristic rising frequency versus time structures; although the temporal variations may appear unusually slow, *Burtis and Helliwell* [1976] have described observations of similar emissions in the earth's magnetosphere. The detailed structure of the Saturnian chorus is displayed in the central panel of Plate 2. (Note: Plate 2 is shown here in black and white. The color version is shown in a separate section of the journal.) Figure 9 and Plate 2 show that the chorus bandwidth is several hundred Hertz and that the amplitude is orders of magnitude greater than that for any of the $(n + \frac{1}{2})f_c$ modes.

At Jupiter, *Scarf et al.* [1979] and *Thorne and Tsurutani* [1979] demonstrated that the measured whistler mode turbulence would produce significant losses of radiation belt electrons. Subsequently, *Coroniti et al.* [1980] identified Jovian chorus, and they showed that these waves precipitate into the atmosphere about 6 ergs/cm^2 s of electrons with energies on the order of a few keV. Thus, it has been established that at Jupiter

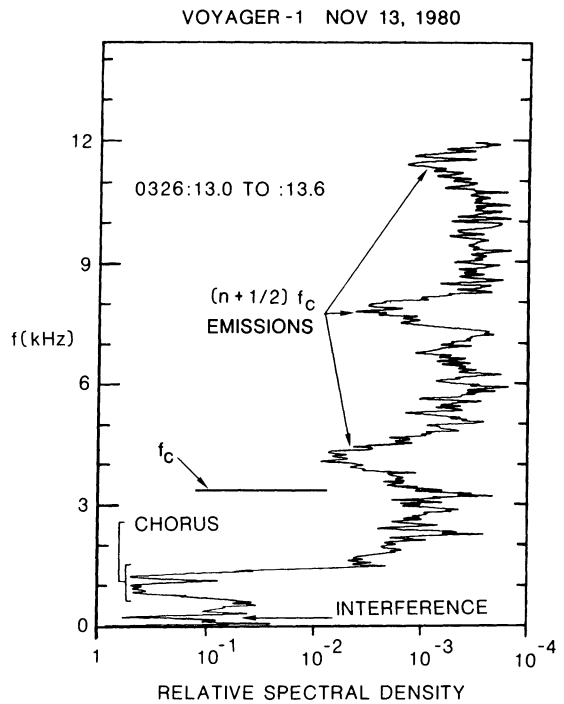

Fig. 10. A spectral density plot constructed from the Voyager 1 waveform data.

pitch angle diffusion and precipitation associated with whistler mode wave-particle interactions are dynamically important, and since we have identified chorus at Saturn, it is necessary to conduct a similar analysis of these new interactions.

For the quantitative analysis we consider the measurements at 0326 and focus attention on the 1-kHz channel. Whistler mode waves that propagate parallel to the B field have an index of refraction (n) given

$$n^2 = 1 + \frac{{f_p}^2}{f(f_c - f)} \tag{1}$$

and since at 0326, B was 120γ, while N was near 20 cm^{-3} (E. C. Sittler, private communication, 1982), we find $f_c = 3.36$ kHz, and $f_p = 40.25$ kHz so that n(1 kHz) ≈ 26. The measured average E field amplitude at 1 kHz was 1.76×10^{-6} V/m(Hz)$^{1/2}$, and thus B' (the magnetic field amplitude of the wave) was 1.54×10^{-4} gammas/(Hz)$^{1/2}$.

The whistler mode waves resonate with electrons having [see *Coroniti et al.*, 1980]

$$\frac{v(\text{res})}{c} \cong \frac{f_c - f}{nf} \tag{2}$$

and the resultant diffusion coefficient $D_{\alpha\alpha}$ is

$$D_{\alpha\alpha} \cong \tfrac{1}{4}\left[\frac{e}{mc}\, 10^{-5} B'(f)\right]^2 \cdot \frac{f}{f_c + 2f} \tag{3}$$

For $f = 1$ kHz at 0326, these expressions yield v(res) $= 2.55 \times 10^9$ cm/s, E(res) $= 1.85$ keV, and $D_{\alpha\alpha} = 3.5 \times 10^{-5}$ s^{-1}.

We assume, as in the analysis for Jupiter, that the interaction region extends over two Saturn radii, centered at the magnetic equator, and therefore we estimate the bounce-average precipitation lifetime to be $T_L \approx (\pi L/2)/D_{\alpha\alpha} \approx 2.5 \times 10^5$ s. (The parameter L is the distance, in units of Saturn radii, to the equatorial crossing of the magnetic field line.) The minimum precipitation lifetime is $T_M = 2L^4 R_s/v$ [*Coroniti et al.*, 1980], and this gives $T_M \approx 4000$ s so that T_M/T_L near the Saturn ring plane crossing indicates that the wave-particle interactions produce only weak diffusion and negligible precipitation. In order to assess this result, it is useful to recall that *Coroniti et al.* [1980] found $T_M/T_L \approx 0.3$ for Jovian chorus, while *Scarf et al.* [1979] and *Thorne and Tsurutani* [1979] found $T_M/T_L \approx 0.01$ to 0.2 for Jovian whistler mode hiss. The Saturn weak diffusion result appears to be quite consistent with electron measurements from the Voyager 1 plasma probe. E. C. Sittler (private communication, 1982) provided data that yields J(2.0 keV) $\approx 5 \times 10^5$ electrons/cm^2 s at 0326, while the stable trapping limit is near 10^7 cm^{-2} s^{-1}. Thus we should not expect strong diffusion or large precipitation fluxes. However, there is still a moderate mystery since at earth and at Jupiter we relate the presence of banded chorus to situations in which the resonant flux approaches the stable trapping limit.

6. Dust Impacts Near the Ring Plane and Elsewhere

Scarf et al. [1982] showed that the intense noise levels measured by Voyager 2 in a narrow region centered about the crossing of the ring plane were associated with detection of a large number of brief impulses, and they proposed dust impacts on the spacecraft as the noise source (see also *Warwick et al.* [1982]). Figure 11 contains expanded 16-channel plots for both the Voyager 1 and 2 crossings of the ring plane/magnetic equator, and this figure demonstrates clearly that the Voyager 2 wave enhancements were confined to an extremely short time interval and that they were detected in all of the channels; these results do not resemble the Voyager 1 chorus hiss measurements of Figure 11 since the Voyager 1 intensity peak is very broad on this time scale and the wave enhancements only appear in the lower frequency channels. Another way to compare the Voyager 1 and 2 measurements near the ring plane/magnetic equator involves use of the wideband data, and we refer again to Plate 2. The bottom two panels have the relevant color-coded frequency-time spectrograms, and from this it appears that at the Voyager 2 ring plane crossing we detected a featureless and essentially uniform noise spectrum over the 48-s frame. In fact, both of these displays (Figure 11 and Plate 2) have temporal resolution that is much too low to establish the true nature of the Voyager 2 ring plane observations.

As noted by *Scarf et al.* [1981*a*], in the wideband mode the antenna voltage is measured once per 34.7 μs, and a full-frequency scan is available once per 60 ms. The individual 60-ms scans are then placed side by side to make the frequency-time spectrograms shown in Plates 1 and 2. However, these frequency-time displays are clearly aliased when impulses with time constants small in comparison with 60 ms are detected, and it is then necessary to examine successive individual voltage measurements. *Scarf et al.* [1982] showed such a display for a single dust impact, and they noted that the voltage pulse decayed in a time small in comparison with a microsecond. *Gurnett et al.* [1982*b*] conducted a detailed analysis of the waveform data collected near the Voyager 2 ring plane crossing, and they showed that the peak impulse rate exceeded 500 impacts/s. These measurements were then used to derive estimates of the mass and size distribution for the impacting particles, and a corrected spatial (north-south) profile of the dust particles was also determined.

In the discussion of the Voyager 2 observations, *Scarf et al.* [1982] noted that isolated impact-like signals were present in audio recordings of other wideband frames from the Voyager 1 Saturn encounter, and they speculated that dust impacts were present even at locations far from the rings.

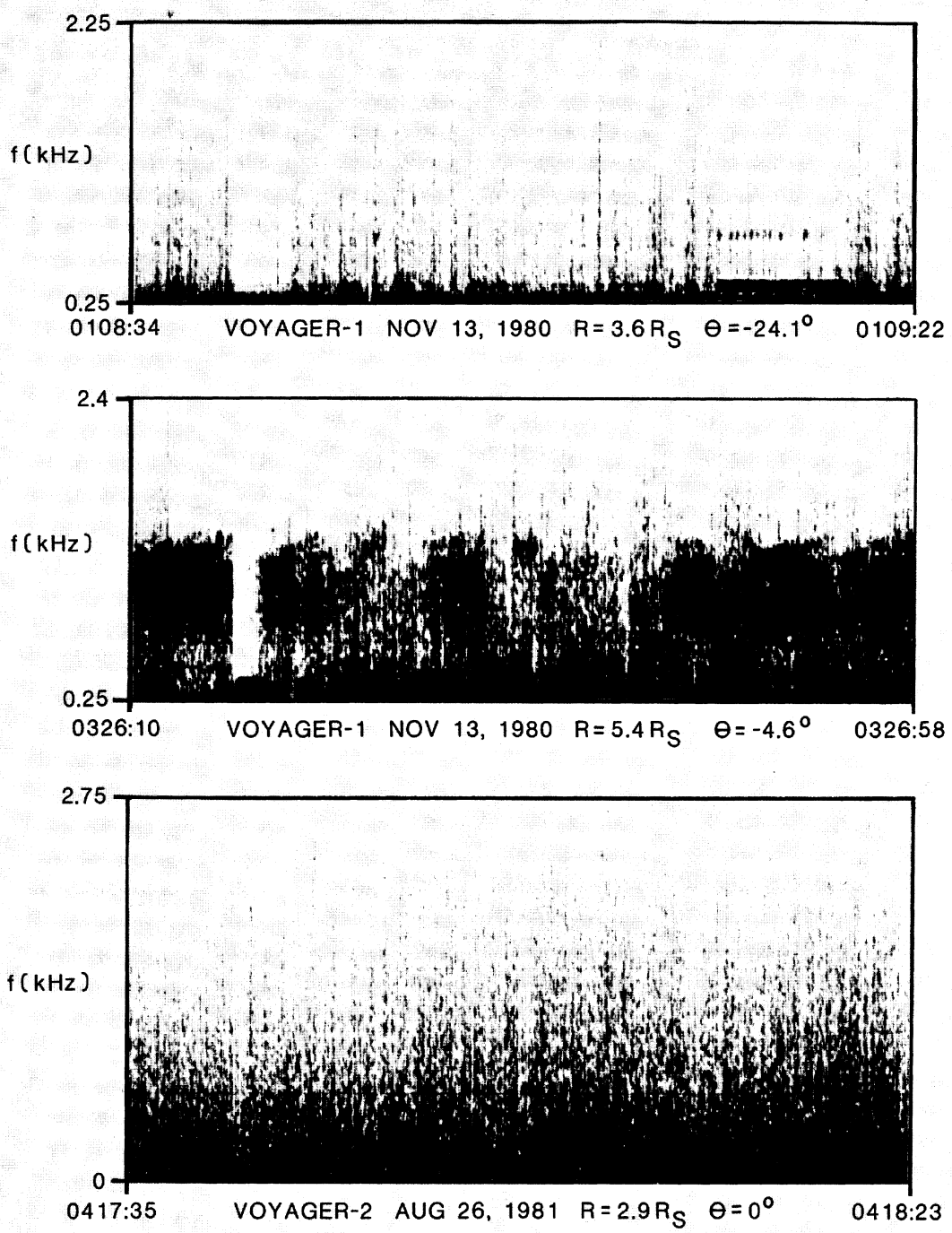

Plate 2. Frequency-time spectrograms from the wideband data. The top panel shows isolated noise spikes during a quiet period near Voyager 1 closest approach (the many low-frequency bursts after 0109:10 are interference signals). The central panel shows Voyager 1 chorus plus impulses. The bottom panel shows the Voyager 2 wideband measurements at the ring plane crossing.

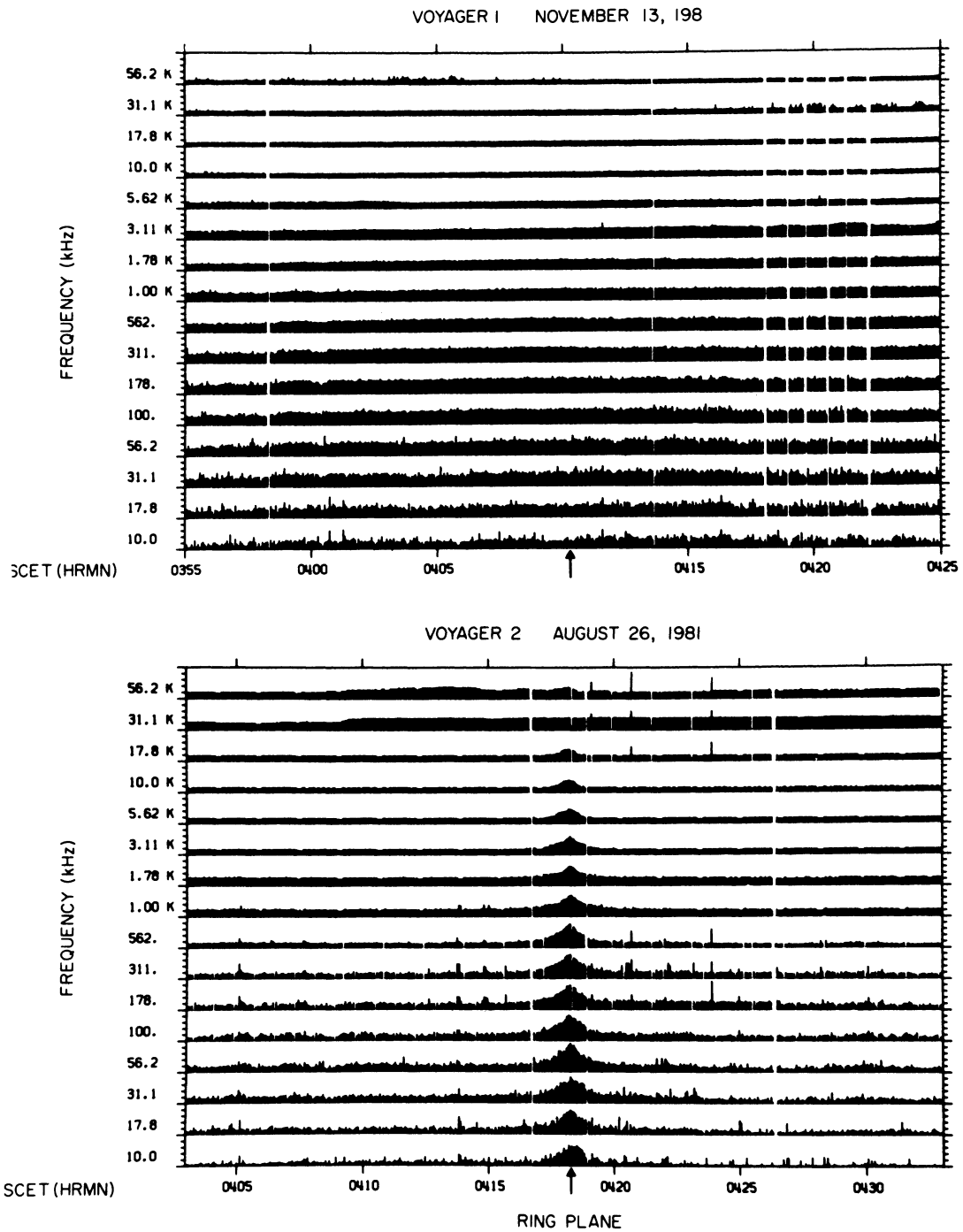

Fig. 11. Comparison of Voyager 1 and 2 16-channel measurements in the vicinity of the ring plane-magnetic equator.

In order to evaluate this speculation, it is necessary to use a more quantitative technique than one based on acoustical evidence, and we refer again to Plate 2. It is clear that the displays for all three of the sequences (including the top one with $\theta \approx -24°$) have vertical lines extending up to at least 1.5 kHz, and these are suggestive of particle impacts (the vertical lines in the range 100–600 Hz that start at 0109:10 in the top panel represent a known spacecraft interference effect and not impacts). In fact, the color-coded displays indicate that a significant difference between the bottom panel and the top two might simply be related to the number of impacts, and this suggests an examination of the highest time resolution measurements.

We have analyzed the 34.7 μs data records for all of these waveform frames, and some characteristic results are displayed in Figure 12. It can be seen that very similar impulses were, in fact, detected on Voyager 1 and Voyager 2. The main differences seem to involve variations in the impulse rates and the related variations in the gain state of the plasma wave automatic gain control amplifier; for the less frequent Voyager 1 impacts, the amplifier was generally in a high or medium gain state between noise bursts, while at the Voyager 2 ring plane crossing the very large impact rate kept the gain state low.

This analysis reinforces the conjecture by *Scarf et al.* [1982] that all of the impulsive signals detected at Saturn by the plasma wave instruments can be explained in terms of dust

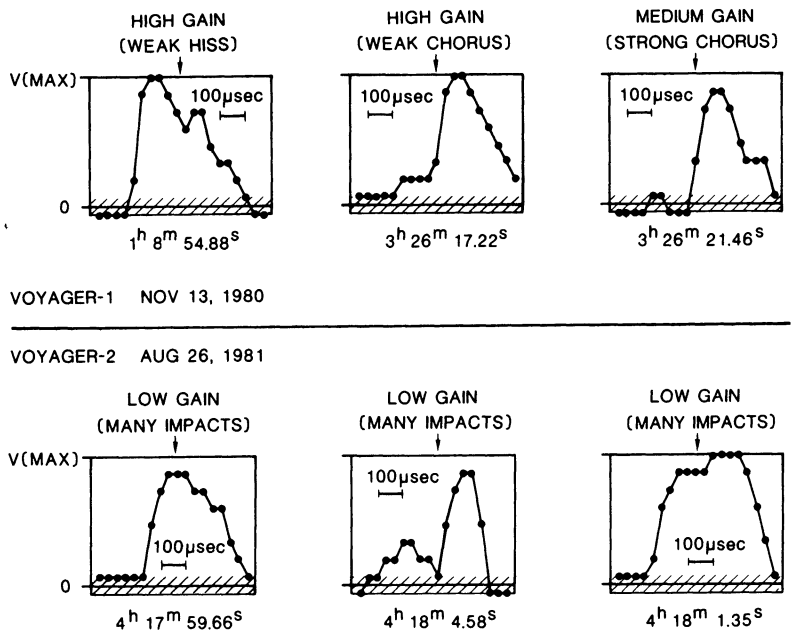

Fig. 12. High-resolution amplitude versus time profiles constructed from the wideband data of Plate 2. We interpret all of these impulses in terms of dust impacts.

impacts. In the initial report, *Scarf et al.* [1982] noted that no such impacts had been found in the Jupiter data, and this preliminary conclusion has also been investigated further; several promising Voyager 1 wideband frames have been examined at the 35 μs resolution for evidence of dust impacts, but no such bursts have been found. It appears that while Saturn's magnetosphere contains dust throughout, Jupiter's does not. It is possible that convection at Jupiter removes charged dust, while the process is not strong at Saturn. However, our conclusion about the absence of dust at Jupiter is still quite preliminary, and evidence for it may yet be found.

The Voyager radio astronomy investigators [*Warwick et al.*, 1981, 1982] have described the detection of another impulsive type of phenomena that occurs only at Saturn, and it is interesting to speculate that there could conceivably be a relation between a subset of these events (called Saturn electrostatic discharges or SEDs) and the plasma wave measurements of dust impacts. The high-frequency SEDs are certainly electromagnetic noise bursts, and we do not suggest any relationship for these. However, for $f \lesssim 100$ kHz, there appear to be few SED events, and in fact, *Kurth et al.* [1982*c*] reported that the plasma wave investigators were unable to detect any SEDs at or below 56 kHz. The only impulsive signals detected by the plasma wave instruments at Saturn are of the dust impact type, and it is possible that such impacts could induce plasma sheath effects that would generate responses up to 100 kHz for a radio system utilizing a monopole antenna.

7. Discussion

The Voyager missions to Jupiter and Saturn were designed to provide opportunities for comparison of phenomena and processes at the two planets. In retrospect we find that these comparisons cannot be made equally in all areas of investigation because the phenomena themselves or the Voyager measurement capabilities were significantly different at Jupiter and Saturn. In this report we have tried to emphasize those variations in the overall science return associated with proximity to Jupiter's tail (for Voyager 2) and those associated with the very different types of magnetic latitude coverage. At Saturn we also had much shorter encounters, with relatively few opportunities to record wideband frames. Nevertheless, it must be recognized that we did obtain enough data to determine that at least some of the dynamical processes are intrinsically different at Jupiter and Saturn. For example, we note that chorus was detected at both planets. However, the flux of resonant electrons at Saturn was so far below the stable trapping limit that the associated precipitation and atmospheric energy input was negligible, while at Jupiter the high fluxes and rapid scattering yield very significant precipitation. In another area, we note that while both Jupiter and Saturn have rings, we only detected phenomena associated with dust impacts during the Saturn encounters. Moreover, we observe that although continuum radiation was detected at both planets, at Saturn the wave levels were so low that the measurements could not be used to evaluate the local plasma densities.

The descriptive phase for the Voyager Saturn encounters is now approaching completion. Future reports will focus attention on multi-instrument correlation studies and on attempts to explain why so many of the magnetospheric measurements appear to indicate that different processes dominate at Jupiter and at Saturn.

Acknowledgments. We are grateful for the support we received from the Voyager project at JPL and at NASA headquarters. We also extend our special thanks to E. Miner and J. Diner of JPL for their efforts in improving the wideband coverage and to P. Jepson and G. Garneau for developing the color spectrogram processing. The excellent data processing efforts of A. Cowen of TRW and the programming support provided by R. West and R. Brechwald of the University of Iowa are also gratefully acknowledged. We gratefully thank H. Bridge, L. Burlaga, F. Coroniti, S. Krimigis, R. Lepping, N. Ness, and J. Warwick for helpful discussions. We are also particularly grateful to A. Lazarus and E. Sittler for providing the latest information on the plasma probe measurements. The research at TRW was supported by NASA through contract 954012 with JPL. The research at the University of Iowa was supported by NASA through contract 954013 with JPL and through grant NGL-16-001-043 with NASA headquarters.

The Editor thanks M. L. Kaiser and D. D. Barbosa for their assistance in evaluating this paper.

References

Anderson, R. R., G. K. Parks, T. E. Eastman, D. A. Gurnett, and L. A. Frank, Plasma waves associated with energetic particles streaming

into the solar wind from the earth's bow shock, *J. Geophys. Res.*, *86*, 4493, 1981.
Bridge, H. S., et al., Plasma observations near Saturn: Initial results from Voyager 1, *Science*, *212*, 217, 1981.
Bridge, H. S., et al., Plasma observations near Saturn: Initial results from Voyager 2, *Science*, *215*, 563, 1982.
Burtis, W. J., and R. A. Helliwell, Magnetospheric chorus: Occurrence patterns and normalized frequency, *Planet. Space Sci.*, *24*, 1007, 1976.
Coroniti, F. V., F. L. Scarf, and C. F. Kennel, Detection of Jovian whistler mode chorus: Implications for the Io torus aurora, *Geophys. Res. Lett.*, *7*, 45, 1980.
Desch, M. D., and M. L. Kaiser, Saturn kilometric radiation: Satellite modulation, *Nature*, *292*, 739, 1981.
Greenstadt, E. W., and R. W. Fredricks, Shock systems in collisionless space plasmas, in *Solar System Plasma Physics*, vol. III, edited by L. J. Lanzerotti, C. F. Kennel, and E. N. Parker, p. 5, North-Holland, Amsterdam, 1979.
Gurnett, D. A., W. S. Kurth, and F. L. Scarf, Plasma waves near Saturn: Initial results from Voyager 1, *Science*, *212*, 235, 1981*a*.
Gurnett, D. A., W. S. Kurth, and F. L. Scarf, Narrowband electromagnetic emissions from Saturn's magnetosphere, *Nature*, *292*, 733, 1981*b*.
Gurnett, D. A., F. L. Scarf, and W. S. Kurth, The structure of Titan's wake from plasma wave observations, *J. Geophys. Res.*, *87*, 1395, 1982*a*.
Gurnett, D. A., E. Grün, D. Gallagher, W. S. Kurth, and F. L. Scarf, Micron-size particles detected near Saturn by the Voyager plasma wave instrument, *Icarus*, in press, 1982*b*.
Gurnett, D. A., W. S. Kurth, and F. L. Scarf, Narrowband electromagnetic emissions from Jupiter's magnetosphere, *Nature*, in press, 1982*c*.
Kurth, W. S., D. A. Gurnett, and F. L. Scarf, The control of Saturn's kilometric radio emission by Dione, *Nature*, *292*, 742, 1981*a*.
Kurth, W. S., D. A. Gurnett, F. L. Scarf, R. L. Poynter, J. D. Sullivan, and H. S. Bridge, Voyager observations of Jupiter's distant magnetotail, *J. Geophys. Res.*, *86*, 8402, 1981*b*.
Kurth, W. S., F. L. Scarf, J. D. Sullivan, and D. A. Gurnett, Detection of nonthermal continuum radiation in Saturn's magnetosphere, *Geophys. Res. Lett.*, *9*, 889, 1982*a*.
Kurth, W. S., J. D. Sullivan, D. A. Gurnett, F. L. Scarf, H. S. Bridge, and E. C. Sittler, Jr., Observations of Jupiter's distant magnetotail and wake, *J. Geophys. Res.*, *87*, 10373, 1982*b*.
Kurth, W. S., D. A. Gurnett, and F. L. Scarf, A search for Saturn electrostatic discharges in the Voyager plasma wave data, *Icarus*, in press, 1982*c*.
Kurth, W. S., F. L. Scarf, and D. A. Gurnett, A survey of electrostatic waves in Saturn's magnetosphere, *J. Geophys. Res.*, this issue.
Lepping, R. P., L. F. Burlaga, M. D. Desch, and L. W. Klein, Evidence for a distant ($>8{,}700\ R_J$) Jovian magnetotail: Voyager 2 observations, *Geophys. Res. Lett.*, *9*, 885, 1982.
Ness, N. F., et al., Magnetic field studies by Voyager 1: Preliminary results at Saturn, *Science*, *212*, 211, 1981.
Ness, N. F., et al., Magnetic field studies by Voyager 2: Preliminary results at Saturn, *Science*, *215*, 558, 1982.
Pederson, B. M., M. G. Aubier, and J. K. Alexander, Low-frequency plasma waves near Saturn, *Nature*, *292*, 714, 1981.
Scarf, F. L., Possible traversals of Jupiter's distant magnetic tail by Voyager and by Saturn, *J. Geophys. Res.*, *84*, 4422, 1979.
Scarf, F. L., and D. A. Gurnett, A plasma wave investigation for the Voyager mission, *Space Sci. Rev.*, *21*, 289, 1977.
Scarf, F. L., R. W. Fredricks, L. A. Frank, and M. Neugebauer, Nonthermal electrons and high-frequency waves in the upstream solar wind, 1, Observations, *J. Geophys. Res.*, *76*, 5162, 1971.
Scarf, F. L., F. V. Coroniti, D. A. Gurnett, and W. S. Kurth, Pitch-angle diffusion by whistler mode waves near the Io plasma torus, *Geophys. Res. Lett.*, *6*, 653, 1979.
Scarf, F. L., D. A. Gurnett, and W. S. Kurth, Measurements of plasma wave spectra in Jupiter's magnetosphere, *J. Geophys. Res.*, *86*, 8181, 1981*a*.
Scarf, F. L., D. A. Gurnett, and W. S. Kurth, Plasma wave turbulence at planetary bow shocks: Saturn, Jupiter, Earth, and Venus, *Nature*, *292*, 747, 1981*b*.
Scarf, F. L., W. S. Kurth, D. A. Gurnett, H. S. Bridge, and J. D. Sullivan, Detection of Jupiter tail phenomena upstream from Saturn, *Nature*, *292*, 585, 1981*c*.
Scarf, F. L., D. A. Gurnett, W. S. Kurth, and R. L. Poynter, Voyager-2 plasma wave observations at Saturn, *Science*, *215*, 587, 1982.
Thorne, R. T., and B. T. Tsurutani, Diffuse Jovian aurora influenced by plasma injection from Io, *Geophys. Res. Lett.*, *6*, 649, 1979.
Warwick, J. W., et al., Planetary radio astronomy observations from Voyager 1 near Saturn, *Science*, *212*, 239, 1981.
Warwick, J. W., et al., Planetary radio astronomy observations from Voyager 2 near Saturn, *Science*, *215*, 582, 1982.

(Received November 15, 1982;
revised March 7, 1983;
accepted March 8, 1983.)

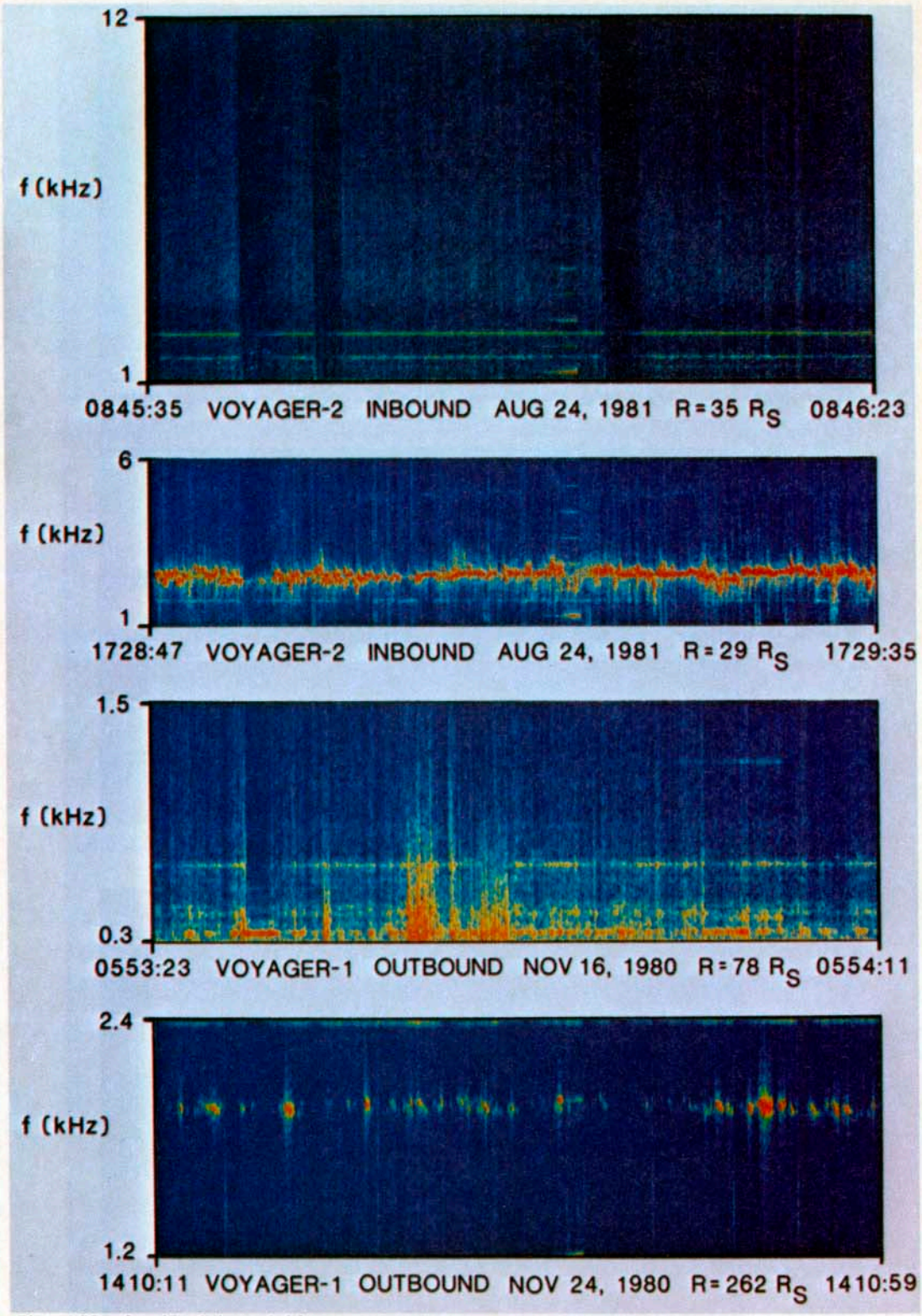

Plate 1 [*Scarf et al.*] Color-coded frequency-time diagrams made up from the wideband measurements. The red tones correspond to the most intense signals, and the blue tones are the weakest ones. The top panel shows weak continuum radiation similar to that detected at Jupiter, and this may indicate that Saturn was near the Jovian tail during the Voyager 2 encounter. The second and bottom panels show electron plasma oscillations, and the other panel shows ion acoustic waves detected at the beginning of the Voyager 1 outbound bow shock traversal.

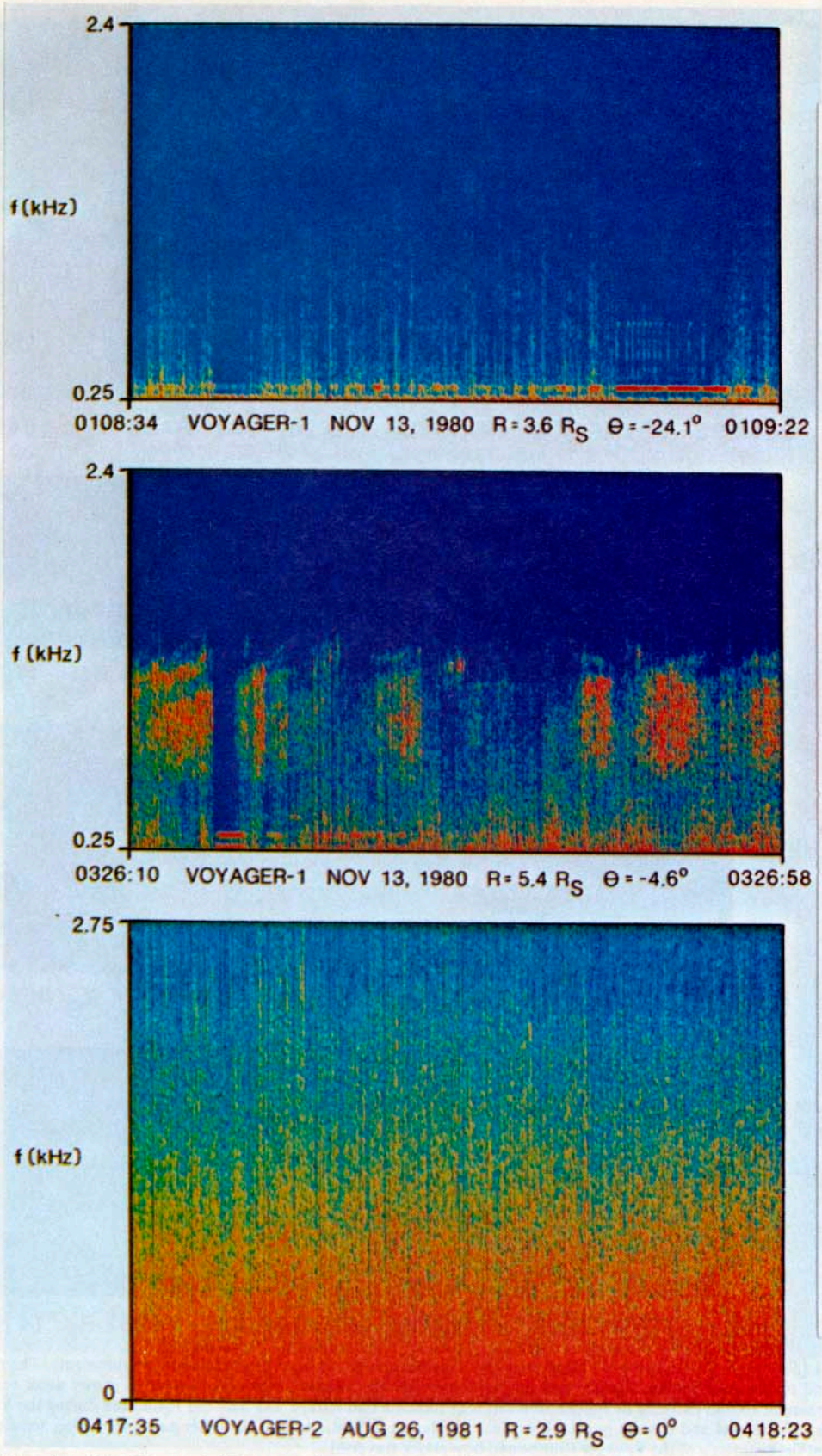

Plate 2 [*Scarf et al.*]. Color-coded frequency-time spectrograms from the wideband data. The top panel shows isolated noise spikes during a quiet period near Voyager 1 closest approach (the many low-frequency bursts after 0109:10 are interference signals). The central panel shows Voyager 1 chorus plus impulses. The bottom panel shows the Voyager 2 wideband measurements at the ring plane crossing.